

Effects of natural gas acidic components on local porosity generation in a carbonate reservoir: Insights from reactive transport modeling

Guanru Zhang, Peng Lu, Pan Luo, Eric Sonnenthal, Yi Huang, and Chen Zhu

AAPG Bulletin, v. 103, no. 12 (December 2019), pp. 2975–3001

Copyright © 2019. The American Association of Petroleum Geologists. All rights reserved.

APPENDIX 1: EFFECTS OF THERMAL CONVECTION ON FLOW FIELD

To investigate whether thermal convection has a large impact on the water flow field for the configuration in this study, we constructed two test cases (“nonisothermal case A” and “nonisothermal case B”), considering heat flow but without transport, reaction, and gas phase invasion processes. The top and bottom boundaries of these two cases are no-flux boundaries with a specified temperature, which is calculated based on the geothermal gradient of 28 °C/km and the Earth’s surface temperature of 15°C (Nathenson and Guffanti, 1987; Wygrala, 1989). The left and right boundary in the nonisothermal case A are no-flux boundaries; therefore, the flow will be controlled only by thermal convection. Left and right boundaries in the nonisothermal case B are similar to the base case; hence, both regional groundwater and thermal convection are involved. Figure S1 shows the spatial distribution of temperature and water flow field when the simulated system reaches a steady state. The flow in the nonisothermal case A is controlled only by thermal convection (the left panel in Figure S1), and the Darcy velocity of the flow is approximately 1.0×10^{-5} m/yr (3.3×10^{-5} ft/yr), which is much smaller than the regional groundwater flow velocity of 1.0×10^{-3} m/yr (3.3×10^{-3} ft/yr). The lower velocity of thermal convection means that in the

nonisothermal case B in which both regional groundwater and thermal convection are involved, the flow field is dominated by the regional groundwater (right panel in Figure S1) and the effect of thermal convection is negligible. These two test cases indicate that neglecting thermal convection is reasonable in our study.

APPENDIX 2: EFFECTS OF CARBONATE FACIES HETEROGENEITY ON LOCAL POROSITY EVOLUTION

To explore the effect of heterogeneity on local porosity, we constructed a simple test case (heterogeneity case). This case considered two carbonate facies (grainstone and packstone) with different porosity and permeability (Grötsch and Mercadier, 1999; Alqattan and Budd, 2017). The distribution of these facies on the anticline reservoir architecture is much simplified (Figure S2A) based on Alsharhan (2006). The porosity and horizontal permeability of the grainstone are 0.1 and 0.4×10^{-13} m² (0.43×10^{-12} ft²), respectively, and the parameter values for the packstone are 0.05 and 0.1×10^{-14} m² (0.11×10^{-13} ft²). Other parameters are the same as the base case.

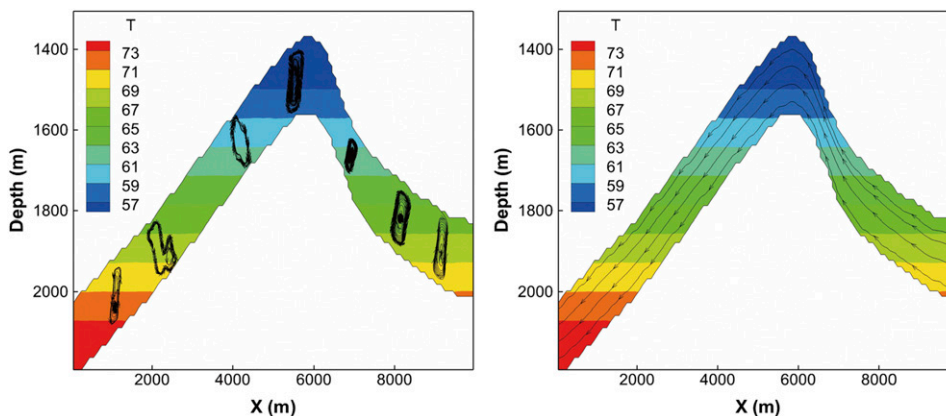


Figure S1. Spatial distribution of temperature (°C) and groundwater stream lines when the simulated system reaches steady state. The left panel is nonisothermal case A and the right panel is nonisothermal case B. T = temperature (°C); X = horizontal distance.

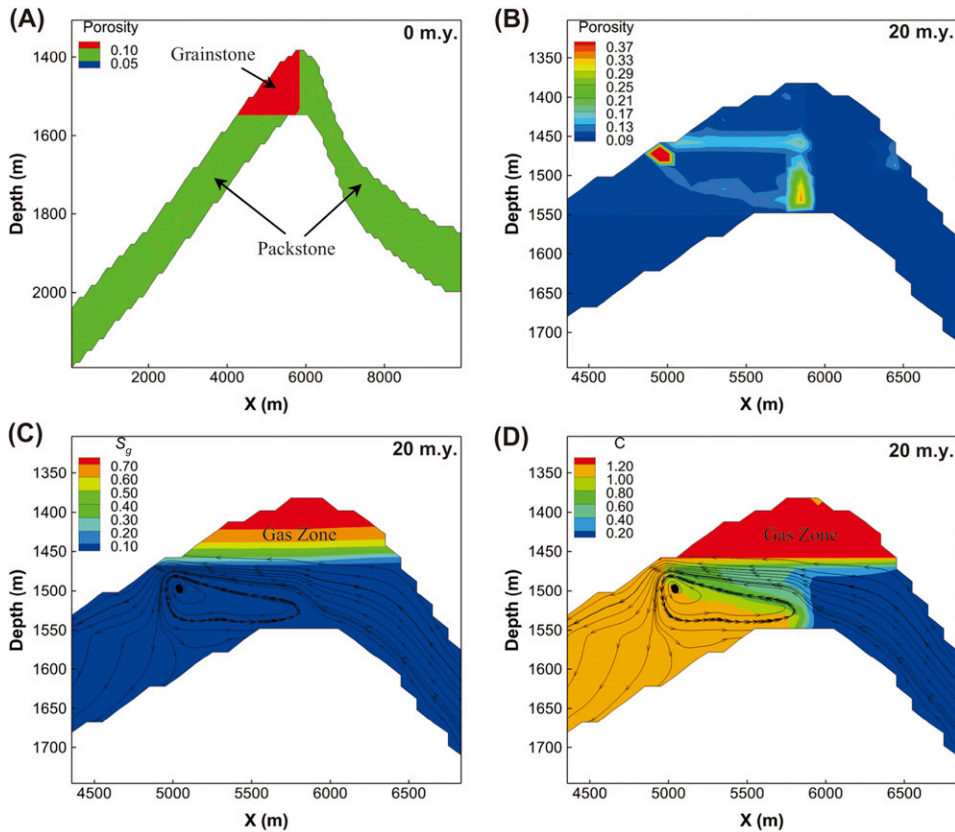


Figure S2. Spatial distribution of (A) facies, (B) porosity, (C) gas saturation (S_g), and (D) C concentration (mol/kg H_2O). The porosity of grainstone is 0.1, and the horizontal permeability is 0.4×10^{-13} (m^2), which is the same as the base case. The porosity of packstone is 0.05 and the horizontal permeability is 0.1×10^{-14} (m^2) [0.11×10^{-13} ft^2]. X = horizontal distance.

The porosity distribution of the heterogeneity case is different from that of the base case (Figure S2B). The local porosity dissolution mainly occurs along the GWC and at the region where the convection and the regional groundwater interact with each other (Figure S2B, D). The maximum secondary porosity is approximately 0.6 (patch shaped near the GWC; Figure S2B), which is much larger than the approximately 0.27 porosity in the base case. Mixing corrosion caused by the interaction between the convection and the regional groundwater is one of the main mechanisms controlling porosity evolution. The local porosity dissolution primarily occurs in the grainstone facies where porosity and permeability are larger than in the packstone (Figure S2A, B). The area of local dissolution in the heterogeneity case is larger than that in the base case in which the dissolution is only mainly along GWC.

The permeability of the packstone is approximately one order smaller than the permeability of the base case, which reduces the Rayleigh number (Farajzadeh et al., 2007; Huppert and Neufeld, 2014) and inhibits the density-driven flow in the right part of the model (Figure S2D). Therefore, the carbon-poor fresh regional groundwater directly contacts the convectational flow with high C concentration at the upper part

of the anticline (Figure S2D). This enhances the fluid-mixing corrosion at the region where the convection and the regional groundwater interact with each other; the generated maximum secondary porosity is approximately 0.23 (Figure S2B).

REFERENCES CITED

- Alqattan, M. A., and D. A. Budd, 2017, Dolomite and dolomitization of the Permian Khuff-C reservoir in Ghawar field, Saudi Arabia: AAPG Bulletin, v. 101, no. 10, p. 1715–1745, doi:10.1306/01111715015.
- Alsharhan, A. S., 2006, Sedimentological character and hydrocarbon parameters of the Middle Permian to Early Triassic Khuff Formation, United Arab Emirates: Geo-Arabia Manama, v. 11, p. 121–158.
- Farajzadeh, R., H. Salimi, P. L. J. Zitha, and H. Bruining, 2007, Numerical simulation of density-driven natural convection in porous media with application for CO_2 injection projects: International Journal of Heat and Mass Transfer, v. 50, p. 5054–5064, doi:10.1016/j.ijheatmasstransfer.2007.08.019.

- Grötsch, J., and C. Mercadier, 1999, Integrated 3-D reservoir modeling based on 3-D seismic: The tertiary Malampaya and Camago buildups, offshore Palawan, Philippines: AAPG Bulletin, v. 83, no. 11, p. 1703–1728.
- Huppert, H. E., and J. A. Neufeld, 2014, The fluid mechanics of carbon dioxide sequestration: Annual Review of Fluid Mechanics, v. 46, p. 255–272, doi:[10.1146/annurev-fluid-011212-140627](https://doi.org/10.1146/annurev-fluid-011212-140627).
- Nathenson, M., and M. Guffanti, 1987, Compilation of geothermal-gradient data in the conterminous United States: Reston, Virginia, US Geological Survey Open-File Report 87-592, p. 1–33.
- Wygrala, B. P., 1989, Integrated study of an oil field in the southern Po basin, northern Italy, Master's thesis, University of Cologne, Cologne, Germany, 217 p.